Original Article

The fusion of tissue spheroids attached to pre-stretched electrospun polyurethane scaffolds

Journal of Tissue Engineering
Volume 5: 1–11

DOI: 10.1177/2041731414556561
tej.sagepub.com
SAGE

Vince Beachley[1], Vladimir Kasyanov[2], Agnes Nagy-Mehesz[3], Russell Norris[3], Iveta Ozolanta[2], Martins Kalejs[2,4], Peteris Stradins[2,4], Leandra Baptista[5], Karina da Silva[5], Jose Grainjero[5], Xuejun Wen[6] and Vladimir Mironov[3,7]

Abstract

Effective cell invasion into thick electrospun biomimetic scaffolds is an unsolved problem. One possible strategy to biofabricate tissue constructs of desirable thickness and material properties without the need for cell invasion is to use thin (<2 μm) porous electrospun meshes and self-assembling (capable of tissue fusion) tissue spheroids as building blocks. Pre-stretched electrospun meshes remained taut in cell culture and were able to support tissue spheroids with minimal deformation. We hypothesize that elastic electrospun scaffolds could be used as temporal support templates for rapid self-assembly of cell spheroids into higher order tissue structures, such as engineered vascular tissue. The aim of this study was to investigate how the attachment of tissue spheroids to pre-stretched polyurethane scaffolds may interfere with the tissue fusion process. Tissue spheroids attached, spread, and fused after being placed on pre-stretched polyurethane electrospun matrices and formed tissue constructs. Efforts to eliminate hole defects with fibrogenic tissue growth factor-β resulted in the increased synthesis of collagen and periostin and a dramatic reduction in hole size and number. In control experiments, tissue spheroids fuse on a non-adhesive hydrogel and form continuous tissue constructs without holes. Our data demonstrate that tissue spheroids attached to thin stretched elastic electrospun scaffolds have an interrupted tissue fusion process. The resulting tissue-engineered construct phenotype is a direct outcome of the delicate balance of the competing physical forces operating during the tissue fusion process at the interface of the pre-stretched elastic scaffold and the attached tissue spheroids. We have shown that with appropriate treatments, this process can be modulated, and thus, a thin pre-stretched elastic polyurethane electrospun scaffold could serve as a supporting template for rapid biofabrication of thick tissue-engineered constructs without the need for cell invasion.

Keywords

Electrospinning, tissue spheroid, tissue fusion, maturogen, pre-stretched scaffold, vascular tissue engineering

Received: 28 July 2014; accepted: 26 September 2014

[1]Department of Biomedical Engineering, Rowan University, Glassboro, NJ, USA
[2]Laboratory of Biomechanics, Riga Stradins University, Riga, Latvia
[3]Department of Regenerative Medicine and Cell Biology, Medical University of South Carolina, Charleston, SC, USA
[4]Department of Cardiac Surgery, Pauls Stradins Clinical University Hospital, Riga, Latvia
[5]Laboratory of Tissue Engineering, Inmetro, Xerém, Rio de Janeiro, Brazil
[6]Department of Chemical and Life Science Engineering, Virginia Commonwealth University, Richmond, VA, USA
[7]Division of 3D Technologies, Renato Archer Center for Information Technology, Campinas, São Paulo, Brazil

Corresponding author:
Vladimir Kasyanov, Laboratory of Biomechanics, Riga Stradins University, Riga, LV-1007, Latvia.
Email: kasyanov@latnet.lv

Introduction

Electrospinning is rapidly emerging as a platform technology for the fabrication of new generations of nanostructured scaffolds.[1–3] Studies indicate that electrospun nanoscaffolds may be useful in the biofabrication of vascular tissue engineering constructs.[4–8] Further investigations in this direction have shown that electrospun scaffolds act as excellent biomimetic nanosubstrates for the adhesion and spread of vascular endothelial cells[9] and smooth muscle cells.[5,10] Electrospun scaffolds are, however, difficult to cellularize because they offer only a limited degree of cell invasion. Several new technologies have emerged in an attempt to overcome this limitation, such as the simultaneous electrospinning of encapsulated cells and fibers,[11,12] the combined use of "sacrificial" (rapidly degradable) and nonsacrificial electrospun fibers,[13] the development of bilayered elastomeric scaffolds,[14] and pore micromachining using femtosecond laser ablation.[15] While each of these methods shows early promise, further investigation into the effective cellularization of electrospun scaffolds remains a justifiable endeavor. One possible strategy to circumvent this issue is to use thin electrospun scaffolds as templates for self-assembling fusogenic (capable of tissue fusion) tissue spheroids. Thin elastic electrospun scaffolds are suitable to provide structure and support to enable rapid fusion of individual cell spheroids into tissue constructs of desirable thickness, while retaining physical and handling properties that are practical for subsequent biofabrication into higher order tissue structures. Moreover, the high porosity and limited thickness of the nanofiber scaffold will allow for continuous direct cell–cell contact between each layer in contrast to bulk material templating approaches.[16]

Tissue spheroids are cell aggregates of sphere-like shape that provide the highest possible initial cell density for tissue engineering and are therefore useful as three-dimensional (3D) building blocks for solid scaffold-free tissue engineering.[17–19] Experiments show that two closely placed tissue spheroids fuse into one new spheroid of larger diameter.[20,21] This process, named tissue fusion, is a ubiquitous process during embryonic development[22] and can be referred to as a biomimetic approach to tissue engineering.[23,24] The fusion of tissue spheroids is a fundamental biological principle and biophysical basis of the emerging bottom-up solid-scaffold-free tissue engineering approach. Tissue spheroids have since been implemented in the fabrication of myocardial tissue,[25–28] nervous tissue,[29,30] and other tissues. More recent studies show that tissue spheroids could be useful in vascular tissue engineering[17] and that vascular tissue spheroids and rods could be used to form the branched segments of vascular tree.[31,32] It has also been demonstrated that liver tissue spheroids can be attached and immobilized on electrospun nanofiber matrices.[33]

Tissue fusion is driven by surface tension forces and is most effective within a hanging drop or fluid environment. The fusion of tissue spheroids can also occur in hydrogels or extracellular matrix substrates; however, the process is strongly dependent on the properties of these substrates.[34] The behavior of tissue spheroids and, more specifically, the tissue fusion processes of vascular tissue spheroids attached to an electrospun scaffold have not yet been systematically investigated. We hypothesize that electrospun scaffolds could be used as temporal support templates for vascular tissue spheroids in the assembly of vascular tissue. Thus, the goal of this study was to evaluate electrospun scaffolds as support templates for rapid tissue fusion–mediated vascular tissue spheroid bioassembly into tissue constructs. The secondary objective is to demonstrate the potential of this approach for subsequent biofabrication of higher order tissue structures, especially in vascular applications. Mechanically biomimetic prestretched elastic electrospun polyurethane (PU) nanofibers have been selected as supporting scaffold. Nanofiber tension present in the pre-stretched electrospun scaffolds allows for very thin nanofiber meshes to support multicellular spheroids with minimal deformation. The elasticity of the electrospun PU scaffolds is essential for subsequent biofabrication of templated fused spheroids into higher order structures and for bioreactor-based biomechanical conditioning of vascular tissue-engineered constructs. Tissue spheroids were derived from human adipose tissue–derived stem cells (ADSCs) as a clinically relevant cells source. ADSCs have been used because they represent an autologous cell source with proven capacity to be directly differentiated into smooth muscle cell lineage and can be isolated during very short time in large amounts from patient's liposucted adipose tissue using commercially available clinical sorters. Potent fibrogenic factor tissue growth factor (TGF)-β1 has been used to enhance the material properties of tissue-engineered constructs by inducing extracellular matrix deposition.

The novel data presented in this article demonstrate that pre-stretched electrospun PU scaffolds can interfere with tissue fusion and the bioassembly of tissue spheroids into tissue-engineered constructs. The data also indicate that a combination of solid scaffold–based and tissue spheroid–based tissue engineering approaches is feasible and offers new and exciting opportunities for self-directed tissue assembly. The dynamics of electrospun scaffold–tissue spheroid interactions are more complex than originally expected; however, scaffold–spheroid interactions could be optimized and balanced by using TGF-β1 treatment. Thus, further study into the visualization and measurement of the physical forces controlling the tissue spheroid fusion process on pre-stretched PU scaffolds is warranted.

Materials and methods

Cell culture

ADSCs (Invitrogen) were re-expanded in MesenPRO RS Basal Medium (Invitrogen) and supplemented with

MesenPRO RS Growth Supplement (Invitrogen), 1% Penicillin/Streptomycin (Invitrogen), 1% L-glutamine (Invitrogen, USA), and 1% AmphotericineB (Invitrogen). Cells were maintained in a humidified incubator at 37°C in 5% CO_2–95% air atmosphere and new media every second day. Cells from the third passage were used for tissue spheroid biofabrication.

Tissue spheroid biofabrication

Tissue spheroids were fabricated in the conventional hanging drop method.[35] Cells were harvested from confluent monolayers by treatment with 0.25% Trypsin/ethylenediaminetetraacetic acid (EDTA) for 5 min in a humidified incubator. The cells were counted and the concentration of the cell suspension was adjusted to 10^6 cell/mL (25,000 cell/25 mL). Droplets of 25 mL were placed on the lids of Petri dishes that were inverted and incubated at 37°C. After 48 h of incubation, the cells were self-assembled into tissue spheroids at the bottom of the droplets by gravitational force.

Scaffold fabrication

PU (Tecoflex SG-80A; Noveon, Cleveland, OH, USA) was dissolved in hexafluoro-2-propanol (HFIP; Oakwood, West Columbia, SC) at a concentration of 8% (wt/v). The solution was electrospun through a blunt tipped 21G needle at a voltage of 10 kV, flow rate of 0.015 mL/min, and drop height of 11 cm. Fibers were collected in aligned arrays of 7-cm-long nanofibers across a polycarbonate rack using a custom-built collection device.[36] The device utilizes two parallel mobile tracks to collect aligned fiber arrays and pull them down to a secondary collecting area at a vertical speed of 10 mm/s. Four single-layer aligned nanofiber sheets collected at 7.5-min intervals were fixed to a square polycarbonate rack oriented in a 90° criss-crossed pattern. Scaffolds were sterilized in 1N HCl for 30 min.

Scanning electron microscopy

Samples were sputter coated with gold at a thickness of 50–70 nm using a Cressington 108 AUTO sputter-coater with a current of 30 mA for 2 min. Images of the samples were taken at 500–10,000 times magnification using a scanning electron microscope (SEM; Hitachi TM-1000, Japan).

Tissue spheroid fusion experiments

Tissue spheroids biofabricated using hanging drop method were manually placed on electrospun PU scaffold; 1, 2, 3, 7, and 50 spheroids were placed as separated clusters. The plastic frame comprising the electrospun scaffold and the attached tissue spheroids were placed in Petri dish with cell culture media. The kinetics of tissue spheroid attachment, spreading, and fusion were monitored daily using an inverted light microscope. Tissue spheroids have been photographed every day after their seeding on electrospun matrices during 1 week.

Biofabrication of tissue-engineered construct

Tissue-engineered constructs suitable for biomechanical testing were biofabricated from self-assembling tissue spheroids cultured on electrospun scaffolds that were specially designed to be very thin and compliant. The average thickness of tissue constructs was 20 ± 3 μm. The average thickness of the PU electrospun scaffold was 1.68 ± 0.82 μm, and interfibrillar space was 10.6 ± 4.3 μm. Approximately 1000 tissue spheroids were placed on each scaffold in standard place. Supporting frames with attached tissue spheroids were placed in Petri dishes. Tissue spheroid fusion kinetics were analyzed using an inverted light microscope. Specific areas of standard size were randomly selected and photographed under standard magnification for morphometric analysis. The constructs were incubated in TGF-β1 up to 2 weeks in order to investigate the feasibility of accelerated tissue maturation. A total of 1000 tissue spheroids were placed on one frame containing electrospun PU scaffold for morphometric, biomechanical, and biochemical analysis. The number of tissue spheroids (1000) was calculated and selected based on the need to biofabricate tissue-engineered construct of minimal sufficient size to be suitable for existing standard method of biomechanical testing using standard equipment. At least five frames were used for every experiment. Tissue spheroids were also placed on non-adhesive hydrogel (agarose) as a control where formation of continuous (pore-free) tissue construct was observed.

Morphometric analysis of tissue-engineered construct

The holes in the tissue-engineered constructs were analyzed using two morphometric parameters: the number of holes per unit of area and the distribution of hole diameter. The number of holes was calculated on unit of standard area at standard magnification. The maximal diameter of hole was measured on large magnification. Five specimens were analyzed from both the control and the TGF-β1 treated groups after 1-week incubation. The light microscopy photographs were taken under standard magnification.

Biomechanical testing

The biomechanical properties of the tissue-engineered construct (force–elongation relationship) with and without TGF-β1 treatment were estimated. Tissue specimens were glued between two fine waterproof sandpaper 1500-b frames (Figure 1) using rubber cement (acid free). Two cuts were made along each side of each specimen.

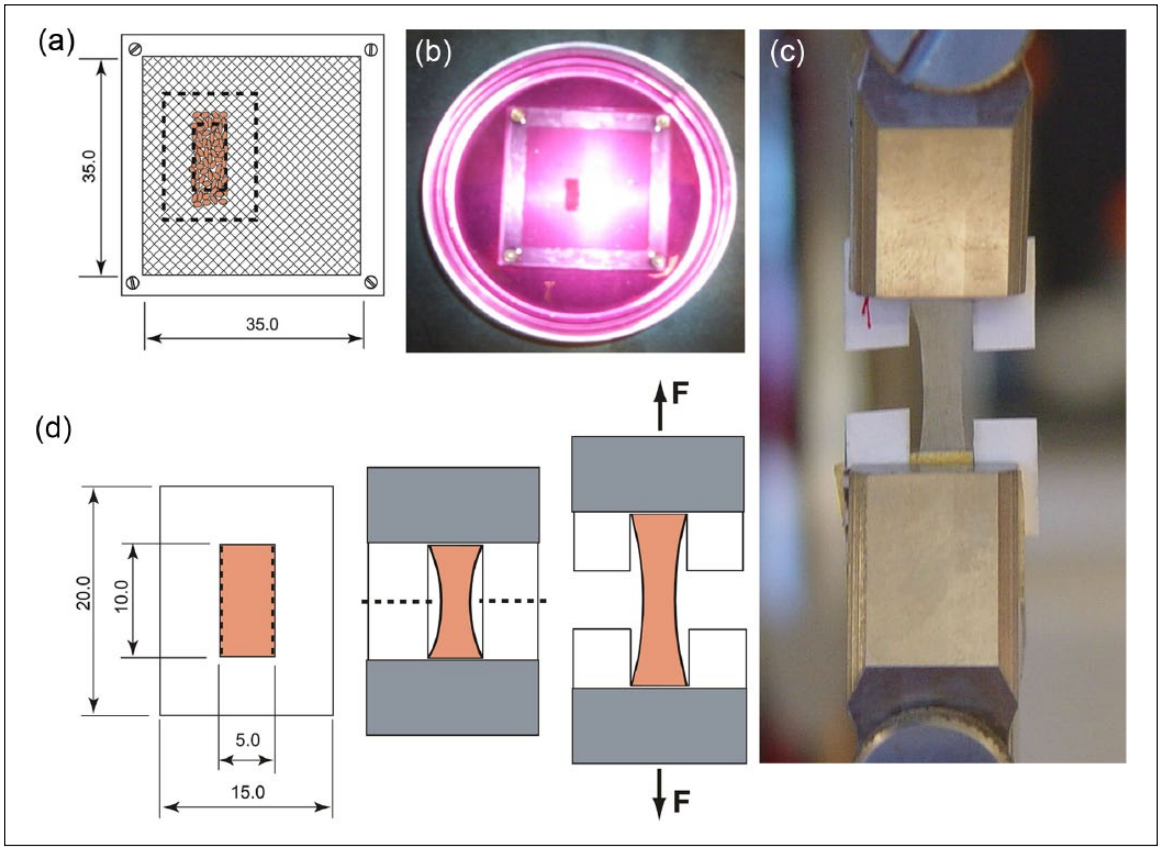

Figure 1. Scheme demonstrating the biomechanical testing procedure: (a) frame with scaffold and tissue spheroids (all dimensions in mm); (b) plastic frame supporting the electrospun polyurethane scaffold in Petri dish—the tissue spheroids do not fall through the scaffold; (c) tensile test of tissue construct sample; and (d) tissue construct sample preparation for tensile test (all dimensions in mm).

The length and width of the each specimen in the frame was 10 and 5 mm, respectively. Tissue specimens were gripped at both ends with two-piece clamps that were lined with sandpaper such that the edges of the frame aligned with the end of the grips. Tensile tests were performed at room temperature (20°C ± 1°C) using a Bose ElectroForce® 3200 Test System with load cell 50 N (Figure 2(b)). The frame improved traction of the tissue within the grips and prevented slippage during the test. The side faces of the frame were cut after the specimens were placed between the grips and the testing machine (Figure 1). Each specimen was loaded at a rate of 0.2 mm/s until they ruptured (this elongation rate usually is used for quasi-static tensile testing of soft biological tissue and biomaterials), and the force-elongation curves were recorded.

Western blotting

Tissue-engineered constructs biofabricated from fused tissue spheroids were collected and lysed in standard radioimmunoprecipitation assay (RIPA: 50 mM Tris pH7.4, 150 mM NaCl, 2 mM EDTA, 1% NP-40, 0.1%SDS, 0.5% sodium deoxycholate) buffer. Protein lysates were electrophoresed and Western blotting was performed with α-collagen antibody (R&D Systems–Minneapolis, MN, USA), α-periostin (Abcam, Cambridge, MA, USA), or α-actin (Santa Cruz, Dallas, TX, USA). Detection was performed using the Femto-ECL detection kit (Pierce, Rockford, IL, USA).

Statistical analysis

Quantitative data were expressed as mean values plus one degree of standard deviation. A total of five specimens were analyzed from each group. The descriptive summary statistics are presented in terms of means and standard deviations. A p value of less than 0.05 was considered statistically significant. Analysis that compared only two groups was conducted using student t-tests with a p value of less than 0.05 to indicate statistical significance.

Results

Characterization of pre-stretched electrospun PU scaffold

Scanning electron microscopy demonstrated that the fibers were oriented perpendicularly to form a dense fibrous meshwork comprising fibers of variable diameter

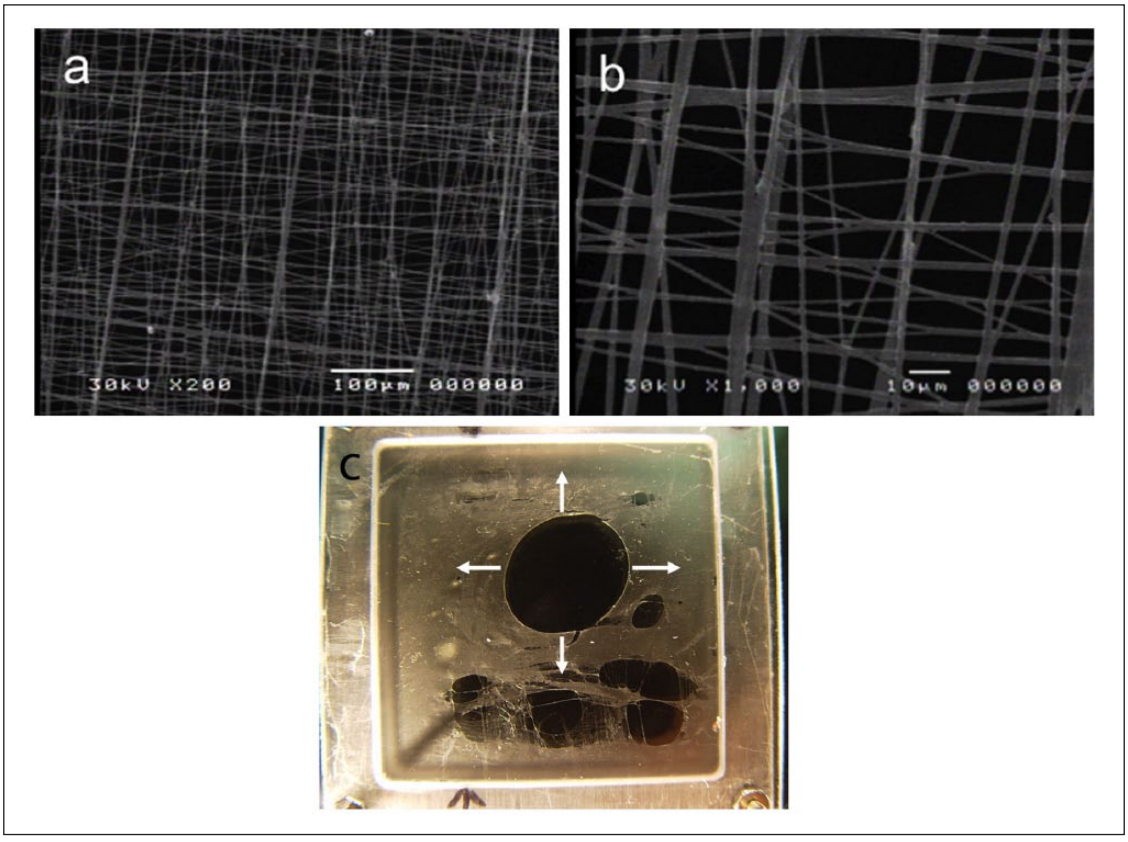

Figure 2. Pre-stretched electrospun polyurethane scaffold: (a) scanning electron microscopy of the electrospun scaffold (small magnification); (b) scanning electron microscopy of the electrospun scaffold (large magnification); and (c) hole formation in the pre-stretched electrospun polyurethane scaffold after rupture—white arrows indicate the centrifugal direction of stretch.

(Figure 2(a) and (b)). The interfibrillar space is small enough to prevent the tissue spheroids from falling through the electrospun scaffold (Figure 2(b)). The immediate formation of rounded holes after the rupture of the microfibrous meshwork is a clear indication that the electrospun scaffold was pre-stretched/under tension (Figure 2(c)). It is logical to assume that the tensions in the scaffold were the result of the drying of the electrospun PU fibers fixed to the rigid plastic support frames or induced by electrical forces during electrospinning. Attempts to cut out the pre-stretched scaffold from the frame resulted in an immediate collapse of the delicate pre-stretched microfibrillar meshwork.

Tissue spheroid adhesion and fusion on pre-stretched electrospun PU scaffold

Tissue spheroids do not fall through the electrospun scaffold due to their relatively large size (300–400 µm) and therefore attached and spread on the scaffold surface (Figure 3). Two, three, and seven closely placed tissue spheroids attached to the electrospun scaffold and underwent fusion to form a thick confluent tissue layer (Figure 3(a)–(c)). Therefore, small tissue-engineered constructs could be biofabricated from a small number of tissue spheroids to form a confluent tissue layer without any holes. It has also been demonstrated that tissue spheroids can not only attach but also spread on electrospun matrices and change orientation of nanofibers by imposing traction forces (Figure 3(d)). Scanning electron microscopy demonstrates close interaction of tissue spheroids with electrospun matrices and incorporation of some electrospun fibers (Figure 3(e)). However, the fusion of 50 closely placed tissue spheroids attached to an electrospun scaffold resulted in the formation of a non-confluent tissue layer with holes of different diameters and shape (Figure 4(a) and (b)). The addition of second and third layers of tissue spheroids did not eliminate or close these observed holes. Moreover, in this case, the preexisting holes evolved into larger crater-like structures (Figure 4(c)). Increasing the cultivation time to 2 weeks also failed to eliminate the holes. Tissue spheroids placed on pre-stretched electrospun porous PU scaffolds fuse into tissue-engineered constructs with pores or one perforated tissue layer of fused tissue spheroids. The appearance of holes strongly correlates with an increased number of tissue spheroids forming the tissue construct.

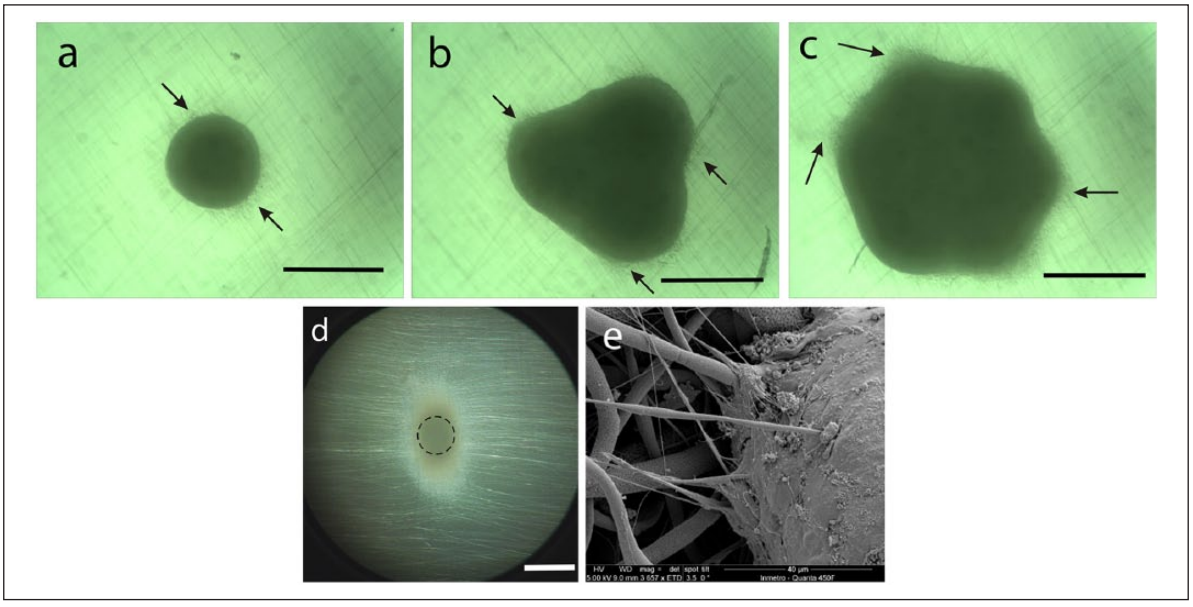

Figure 3. Tissue spheroids behavior on pre-stretched electrospun polyurethane scaffolds. (a) Single tissue spheroids attached to the electrospun polyurethane scaffold (arrows indicate the areas of attachment-dependent cell and tissue spreading). Scale bar—300 μm. (b) Three fused tissue spheroids attached to the electrospun polyurethane scaffold (arrows indicate the areas of attachment-dependent cell and tissue spreading). Scale bar—300 μm. (c) Seven fused tissue spheroids attached to the electrospun polyurethane scaffold (arrows indicate the areas of attachment-dependent cell and tissue spreading). Scale bar—300 μm. (d) Tissue spheroid on electrospun polyurethane scaffold. Tissue spheroid imposes traction forces on electrospun scaffold and changes original orientation of polyurethane fibers in centripetal direction. The original size and counters of tissue spheroid before spreading are outlined by dotted line. Scale bar—300 μm. (e) Adhesion of tissue spheroids to electrospun matrix—scanning electron microscopy.

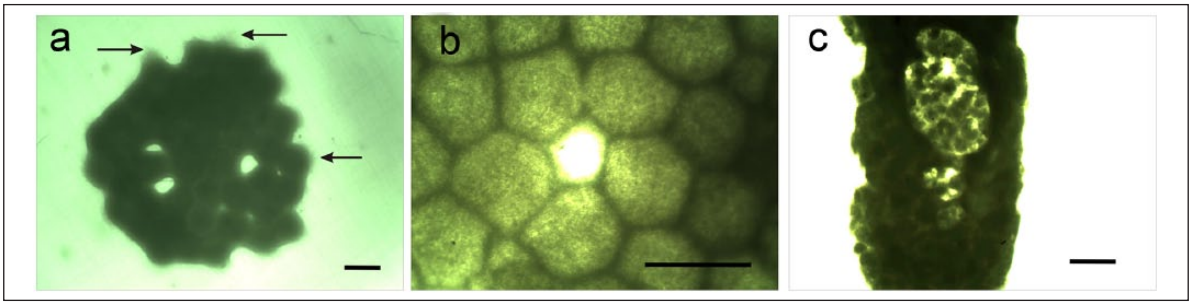

Figure 4. Hole formation during fusion of tissue spheroids attached to pre-stretched electrospun matrix. (a) 50 incompletely fused (with holes) tissue spheroids attached to the electrospun polyurethane scaffold (arrows indicate the areas of attachment-dependent cell and tissue spreading). Scale bar—300 μm. (b) A hole between tissue spheroids that has not completely fused. Scale bar—300 μm. (c) Crater-like structures and persisted defects in the tissue construct after the addition of sequential layers of tissue spheroids. Scale bar—1 mm.

Effect of TGF-β1 treatment on the pre-stretched electrospun PU scaffold

Potent fibrogenic factor TGF-β1 capable of inducing extracellular matrix synthesis and deposition as well as contractile phenotype in employed human ADSCs was used to eliminate holes and mature the tissue constructs. In order to estimate the effect of TGF-β1 treatment on material properties of tissue-engineered constructs, biomechanical testing was performed using cell-free electrospun scaffolds and tissue spheroid seeded electrospun scaffolds (but without TGF treatment) and as controls. The use of TGF-β1 dramatically reduced the number and diameter of the holes (Figure 5). The number of holes reduced from 3.4 ± 0.6 to 1.9 ± 0.3 ($p < 0.05$), and the diameter of holes reduced from 229 ± 63 to 110 ± 24 ($p < 0.05$) (Figure 6). The observations revealed that after TGF-β1 treatment, the remaining tissue spheroids inside tissue-engineered constructs were more regularly packed. Moreover, the incubation with the TGF-β1 resulted in an increased maximal load and stiffness of tissue-engineered

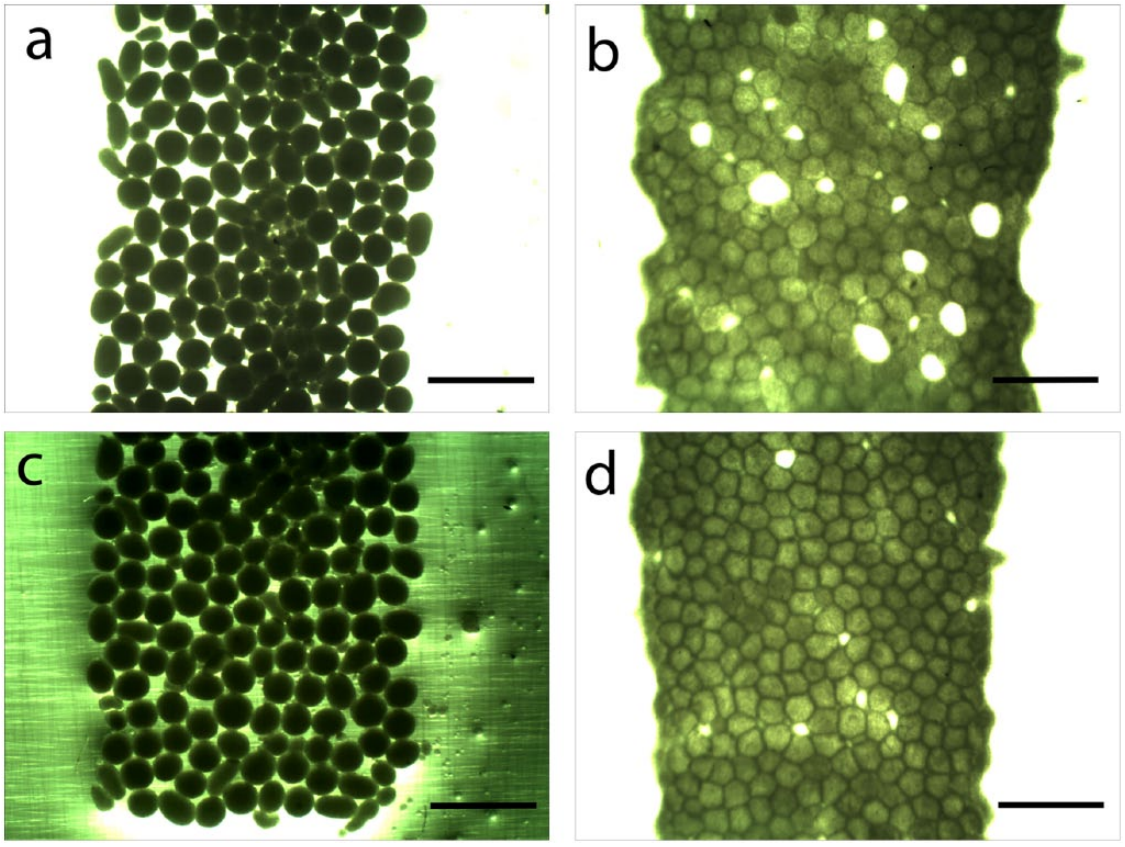

Figure 5. Formation of holes in tissue constructs as a result of incomplete tissue spheroids fusion on pre-stretched electrospun matrix and their dramatic reduction after TGF-β1 treatment. (a) Tissue spheroids placed on electrospun polyurethane scaffold before tissue fusion and without TGF-β1 treatment (control). Scale bar—1 mm. (b) Large holes in the fused tissue construct are formed on the pre-stretched electrospun polyurethane scaffold without TGF-β1 treatment (control). Scale bar—1 mm. (c) Tissue spheroids adherent to the electrospun polyurethane scaffold before tissue fusion and TGF-β1 treatment (experiment). Scale bar—1 mm. (d) A reduction in the size and density of holes in the fused tissue construct on pre-stretched electrospun polyurethane scaffold after TGF-β1 treatment (experiment). Scale bar—1 mm.
TGF: tissue growth factor.

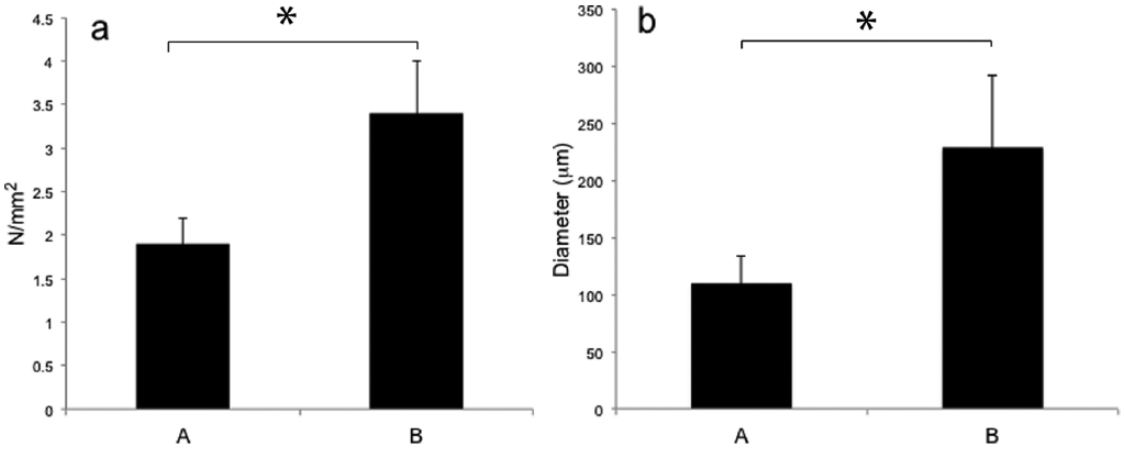

Figure 6. Morphometric analysis of holes in tissue-engineered constructs: (a) number of holes per unit of tissue construct area reduced after treatment with TGF-β1 (A—after TGF-β1 treatment; B—control); (b) diameter of holes in tissue construct dramatically reduced after treatment with TGF-β1 (A—after TGF-β1 treatment; B—control).
TGF: tissue growth factor.
*The difference between values is statistically valid, $p < 0.05$.

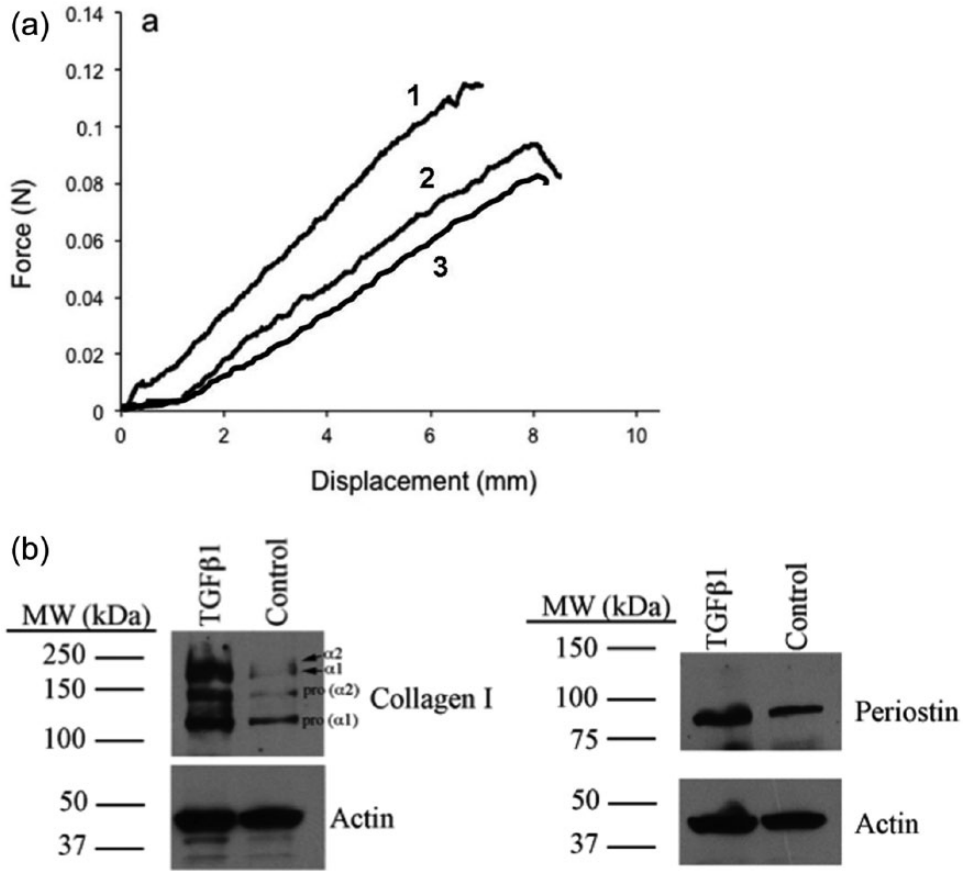

Figure 7. The effects of TGF-β1 treatment on the biomechanical and biochemical properties of the tissue-engineered construct. (a) Force–displacement relationship for samples: 1—tissue construct after TGF-β1 treatment; 2—tissue construct without TGF-β1 treatment; 3—polyurethane scaffold (control). TGF-β1 treatment increases rigidity of tissue constructs. (b) Protein expression of the alpha chains (a1 and a2) as well as pro-collagen precursors (pro-a1, pro-a2) significantly increased after TGF-β1 treatment. The expression of periostin, a known regulator of collagen cross-linking and synthesis, also significantly increased after TGF-β1 treatment. Molecular weight markers (MW) are labeled and Actin was used as a normalization control for protein loading.
TGF: tissue growth factor.

construct (Figure 7(a)). Finally, TGF-β1 was also shown to induce the synthesis of collagen type 1 and the matricellular protein periostin in the tissue-engineered construct (Figure 7(b)).

Elimination of holes in tissue-engineered construct after release from stretch

Two parallel cuts close to the border of the tissue construct were made in the scaffold in order to completely eliminate the tension present in the tissue-engineered construct. Many of the small holes instantly closed or collapsed and the large holes became elongated into an ellipsoid form after the tension was released. This confirmed the presence of tension in the scaffolds throughout the tissue fusion process. From another point of view, even single attached and spread tissue spheroid imposed traction forces on the supporting PU scaffold manifested by changing the original orientation of scaffold fibers (Figure 3(d)). Taken together, these data strongly indicate similarity to in vivo situations where soft tissues are usually pre-stretched/under tension as demonstrated by residual stresses. The observed tissue construct phenotypes are manifestation of balances between two competing forces: traction forces generated by attached, spread, and fused tissue spheroids from one side and forces imposed on tissue constructs by the tension in the pre-stretched nanofibers from another side (Figure 2(c)). Although presented data strongly indicate the existence of competing physical forces operated on tissue–scaffold interface, the visualization, precision mapping, and direct or indirect measuring of these forces are subjects of forthcoming investigations.

Formation of continuous (pore-free) tissue construct from tissue spheroids placed on non-adhesive hydrogel

Tissue spheroids where placed on a non-adhesive hydrogel (agarose), and sequential stages of formation of continuous (hole-free) tissue constructs have been observed (Figure 8).

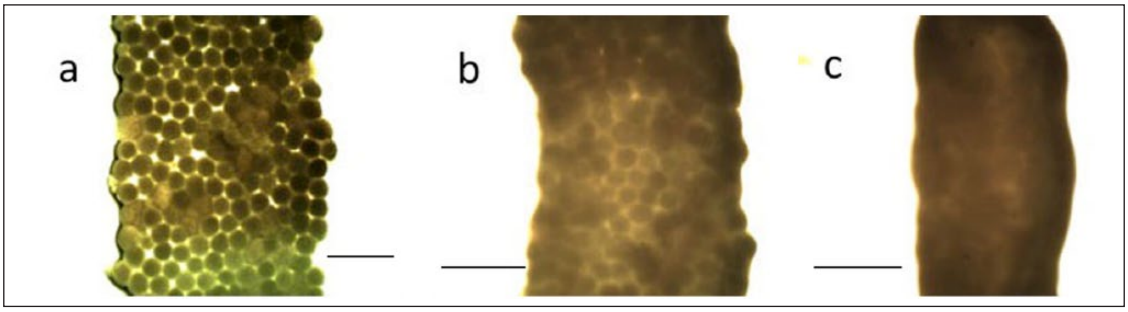

Figure 8. Tissue spheroid fusion on non-adhesive hydrogel (agarose). (a) Tissue spheroids placed on non-adhesive hydrogel (agarose) before tissue fusion. Scale bar—1 mm. (b) Intermediate step of tissue spheroid fusion placed on non-adhesive (agarose) hydrogel. Small holes still persist (24 h after beginning of fusion). Scale bar—1 mm. (c) Complete fusion of tissue spheroids placed on non-adhesive hydrogel (agarose) and formation of tissue construct without any holes or defects (72 h after beginning of fusion). Scale bar—1 mm.

Formation of continuous tissue constructs from fusogenic tissue spheroids non-attached to substrates due to its non-adhesivity was associated with a dramatic reduction of construct size. The experiments with formation of continuous tissue constructs on non-adhesive hydrogel in the absence of attachment of tissue spheroids to a substrate confirm the fact that attachment of tissue spheroids to pre-stretched elastic PU substrate interferes with continuous tissue construct formation due to tethering (attachment and immobilization) effects.

Discussion

The main observation in this study is that tissue spheroids can attach, spread, and form relatively thick tissue layer on thin pre-stretched electrospun PU scaffolds when placed closely together. This study indicates that electrospun scaffolds provide an adhesion permissive surface for tissue spheroids. The observation of incomplete tissue spheroid fusion and the appearance of holes on pre-stretched electrospun PU scaffolds is an interesting and unexpected phenomenon. A logical explanation of the phenomenon is the well-known fact that the fusion of tissue spheroids in closely placed hanging drops results in "new" tissue spheroids that are smaller in diameter than the sum of the diameter of the two "maternal" spheroids. It is also greatly accepted that surface tension is the main force behind tissue spheroid fusion.[18] However, this situation dramatically changes when tissue spheroids are subject to additional "tethering" effects or adhesive forces from the substrate. One could assume that constructs engineered to accommodate the tissue compaction associated with tissue fusion processes[34] would be flexible enough to form a confluent tissue construct. For example, it was shown that hundreds of tissue spheroids could fuse on adhesive collagen substrates without the formation of any holes.[37] However, it is also possible to theoretically argue that as the number of tissue spheroids increases from hundreds to thousands, it will be possible to observe formation of hole defects because collagen hydrogel is attached or fixed to the Petri dish wall or plastic multiwall and, thus, pre-stretched. Finally, it is possible to assume that variability in tissue spheroid size and shape could be responsible for the formation of holes. However, the dense packing of spheres of uniform size in confined space results in the formation of packing defects. It is logical to assume that tissue fusion process unrestricted by "tethering effect" must serve as a biological mechanism to eliminate or prevent any packing defects. Our experiment with tissue spheroid fusion on non-adhesive substrates (such as agarose hydrogel) demonstrates that the use of even thousands of tissue spheroids does not result in any holes or defects. Thus, "tethering effect" induced hole defects likely occurred when tissue spheroids attach to the electrospun nanofiber substrate.

Another significant observation is the demonstration of the "restoration" (hole closing) effects of TGF-β to promote confluency of tissue constructs biofabricated from tissue spheroids on the pre-stretched electrospun PU scaffold. There are at least two theoretical explanations on this effect. The first is that TGF-β could be acting as a potent fibrogenic factor that induces the synthesis of collagen type 1, and other extracellular matrices that result in the increased cohesion of tissue spheroids. Our findings that report an increased synthesis of collagen and periostin support this hypothesis. It has recently been shown that periostin induces collagen fibrillogenesis[38] and acts as a maturogenic factor.[39] It was also recently shown that periostin can contract cell-free collagen hydrogel[40] and that the addition of certain soluble extracellular matrix proteins, such as fibronectin, increases the cohesion (compaction) of tissue spheroids.[41,42] An alternate explanation is that TGF-β could differentiate some stem cells into contractile myofibroblasts and/or smooth muscle cells that then contract tissue constructs. It is widely recognized that TGF-β increases the contraction of fibroblast populated collagen hydrogel[43] and induces the expression of alpha smooth muscle actin—a marker of myofibroblast.[44] However, it is not possible to rule out the synergistic effects of both compaction and

contraction mechanisms. If other "maturogenic" factors impose similar effects on incompletely fused tissue layer of tissue spheroids, then a miniaturized version of this assay could serve as a quantitative in vitro assay for the study of tissue maturation and even offer a new method to high throughput screen maturation factors by the automated image analysis (detection and estimation of the number, density, and size distribution of holes).

Finally, the reported observation that holes instantly disappear when tissue-engineered constructs are cut from the pre-stretched supporting PU scaffold supports the hypothesis that electrospun scaffold nanofiber tension forces are maintained throughout the tissue fusion process and that the interaction between surface tension forces associated with tissue fusion and the adhesive forces between the spheroids and the underlying nanofiber template prevent complete tissue fusion. Moreover, at least practically, it would be impossible to completely eliminate these competing forces in resulted tissue-engineered constructs as long as pre-stretched (or not pre-stretched) electrospun elastic nanofibers and tissue spheroids physically interact and simultaneously impose physical traction forces on each other. Thus, finding a proper balance of these competing physical forces is probably a more realistic option and more practical approach. In this context, an assortment of carefully tailored and calibrated pre-stretched electrospun scaffolds could potentially comprise a technological platform for the study and measure of forces directing tissue spheroid fusion in more complex biomechanical environments. For example, such research tools could be useful for the precise measurement of the surface tension forces generated by fusing tissue spheroids and the scaffold imposed tethering forces interfering with tissue spheroid fusion process.

The flexible elastic and pre-stretched substrates with adhered tissue spheroids undergoing tissue fusion could also be potentially used for the design of self-directed self-assembling or self-folding tissue constructs in emerging four-dimensional (4D) printing and potentially 4D bioprinting technology.[45] Another potential application of pre-stretched PU nanofiber scaffolds could be the use for accelerating tissue maturation by imposing precisely calibrated mechanical stretch on tissue engineering constructs in bioreactor-based mechanical conditioning. Finally, a hybrid compliant scaffold could be designed and fabricated with pre-stretched electrospun PU for the biomimetic tissue engineering of vascular constructs formed from fusogenic vascular tissue spheroids placed on electrospun matrices.

Conclusion

A thin electrospun PU nanofiber scaffold was used as a template for spheroid fusion. Tissue spheroids attached and spread on thin electrospun PU scaffolds and, to a certain degree, will undergo tissue fusion with the formation of a thick confluent tissue layer attached to the scaffold. With increasing number of tissue spheroids, the tissue fusion on pre-stretched electrospun scaffold is incomplete and results in the formation of a tissue layer with hole defects. However, the size and frequency of these holes were dramatically reduced with the addition of maturogenic factors such as TGF-β. Our findings highlight the complexity of the spheroid fusion process on adhesive substrates and demonstrate the potential of nanofiber scaffolds as a tool to measure forces associated with this process. Furthermore, the formation of confluent tissue layers on thin elastic nanofiber scaffolds with factor treatment demonstrates their potential as a template for spheroid fusion and subsequent biofabrication of higher order tissue structures.

Acknowledgements

Vince Beachley and Vladimir Kasyanov contributed equally to this article. Xuejun Wen and Vladimir Mironov contributed equally to this article.

Declaration of conflicting interests

Authors declared no conflict of interest.

Funding

This study has been supported by NSF R-II grant "South Carolina Project for Organ Biofabrication"; Latvia National Research Programme "Development of new prevention, treatment, diagnostics means and practices and biomedicine technologies for improvement of public health"; NIGMS of the National Institutes of Health under award number 5P20GM103444-07; and Brazilian CNPq and FAPESP grants.

References

1. Liao S, Li B, Ma Z, et al. Biomimetic electrospun nanofibers for tissue regeneration. *Biomed Mater* 2006; 1: R45–R53.
2. Pham QP, Sharma U and Mikos AG. Electrospinning of polymeric nanofibers for tissue engineering applications: a review. *Tissue Eng* 2006; 12: 1197–1211.
3. Sill TJ and von Recum HA. Electrospinning: applications in drug delivery and tissue engineering. *Biomaterials* 2008; 29: 1989–2006.
4. Boland ED, Matthews JA, Pawlowski KJ, et al. Electrospinning collagen and elastin: preliminary vascular tissue engineering. *Front Biosci* 2004; 9: 1422–1432.
5. Hashi CK, Zhu Y, Yang GY, et al. Antithrombogenic property of bone marrow mesenchymal stem cells in nanofibrous vascular grafts. *Proc Natl Acad Sci U S A* 2007; 104: 11915–11920.
6. Mironov V, Kasyanov V and Markwald RR. Nanotechnology in vascular tissue engineering: from nanoscaffolding towards rapid vessel biofabrication. *Trends Biotechnol* 2008; 26: 338–344.
7. Wu H, Fan J, Chu CC, et al. Electrospinning of small diameter 3-D nanofibrous tubular scaffolds with controllable nanofiber orientations for vascular grafts. *J Mater Sci Mater Med* 2010; 21: 3207–3215.

8. Xu C, Inai R, Kotaki M, et al. Electrospun nanofiber fabrication as synthetic extracellular matrix and its potential for vascular tissue engineering. *Tissue Eng* 2004; 10: 1160–1168.
9. Uttayarat P, Perets A, Li M, et al. Micropatterning of three-dimensional electrospun polyurethane vascular grafts. *Acta Biomater* 2010; 6: 4229–4237.
10. Stitzel J, Liu J, Lee SJ, et al. Controlled fabrication of a biological vascular substitute. *Biomaterials* 2006; 27: 1088–1094.
11. Stankus JJ, Guan J, Fujimoto K, et al. Microintegrating smooth muscle cells into a biodegradable, elastomeric fiber matrix. *Biomaterials* 2006; 27: 735–744.
12. Stankus JJ, Soletti L, Fujimoto K, et al. Fabrication of cell microintegrated blood vessel constructs through electrohydrodynamic atomization. *Biomaterials* 2007; 28: 2738–2746.
13. Metter RB, Ifkovits JL, Hou K, et al. Biodegradable fibrous scaffolds with diverse properties by electrospinning candidates from a combinatorial macromer library. *Acta Biomater* 2010; 6: 1219–1226.
14. Soletti L, Hong Y, Guan J, et al. A bilayered elastomeric scaffold for tissue engineering of small diameter vascular grafts. *Acta Biomater* 2010; 6: 110–122.
15. Lee BL, Jeon H, Wang A, et al. Femtosecond laser ablation enhances cell infiltration into three-dimensional electrospun scaffolds. *Acta Biomater* 2012; 8: 2648–2658.
16. Yuan B, Jin Y, Sun Y, et al. A strategy for depositing different types of cells in three dimensions to mimic tubular structures in tissues. *Adv Mater* 2012; 24: 890–896.
17. Kelm JM, Lorber V, Snedeker JG, et al. A novel concept for scaffold-free vessel tissue engineering: self-assembly of microtissue building blocks. *J Biotechnol* 2010; 148: 46–55.
18. Mironov V, Visconti RP, Kasyanov V, et al. Organ printing: tissue spheroids as building blocks. *Biomaterials* 2009; 30: 2164–2174.
19. Jakab K, Norotte C, Marga F, et al. Tissue engineering by self-assembly and bio-printing of living cells. *Biofabrication* 2010; 2: 022001.
20. Dean DM, Napolitano AP, Youssef J, et al. Rods, tori, and honeycombs: the directed self-assembly of microtissues with prescribed microscale geometries. *FASEB J* 2007; 21: 4005–4012.
21. Mironov V, Boland T, Trusk T, et al. Organ printing: computer-aided jet-based 3D tissue engineering. *Trends Biotechnol* 2003; 21: 157–161.
22. Perez-Pomares JM and Foty RA. Tissue fusion and cell sorting in embryonic development and disease: biomedical implications. *Bioessays* 2006; 28: 809–821.
23. Marga F, Neagu A, Kosztin I, et al. Developmental biology and tissue engineering. *Birth Defects Res C Embryo Today* 2007; 81: 320–328.
24. Mironov V, Kasyanov V, Drake C, et al. Organ printing: promises and challenges. *Regen Med* 2008; 3: 93–103.
25. Kelm JM, Djonov V, Hoerstrup SP, et al. Tissue-transplant fusion and vascularization of myocardial microtissues and macrotissues implanted into chicken embryos and rats. *Tissue Eng* 2006; 12: 2541–2553.
26. Kelm JM, Djonov V, Ittner LM, et al. Design of custom-shaped vascularized tissues using microtissue spheroids as minimal building units. *Tissue Eng* 2006; 12: 2151–2160.
27. Stevens KR, Kreutziger KL, Dupras SK, et al. Physiological function and transplantation of scaffold-free and vascularized human cardiac muscle tissue. *Proc Natl Acad Sci U S A* 2009; 106: 16568–16573.
28. Stevens KR, Pabon L, Muskheli V, et al. Scaffold-free human cardiac tissue patch created from embryonic stem cells. *Tissue Eng Part A* 2009; 15: 1211–1222.
29. Layer PG, Robitzki A, Rothermel A, et al. Of layers and spheres: the reaggregate approach in tissue engineering. *Trends Neurosci* 2002; 25: 131–134.
30. Rothermel A, Biedermann T, Weigel W, et al. Artificial design of three-dimensional retina-like tissue from dissociated cells of the mammalian retina by rotation-mediated cell aggregation. *Tissue Eng* 2005; 11: 1749–1756.
31. Norotte C, Marga FS, Niklason LE, et al. Scaffold-free vascular tissue engineering using bioprinting. *Biomaterials* 2009; 30: 5910–5917.
32. Visconti RP, Kasyanov V, Gentile C, et al. Towards organ printing: engineering an intra-organ branched vascular tree. *Expert Opin Biol Ther* 2010; 10: 409–420.
33. Chua KN, Lim WS, Zhang P, et al. Stable immobilization of rat hepatocyte spheroids on galactosylated nanofiber scaffold. *Biomaterials* 2005; 26: 2537–2547.
34. Jakab K, Neagu A, Mironov V, et al. Engineering biological structures of prescribed shape using self-assembling multicellular systems. *Proc Natl Acad Sci U S A* 2004; 101: 2864–2869.
35. Kelm JM, Timmins NE, Brown CJ, et al. Method for generation of homogeneous multicellular tumor spheroids applicable to a wide variety of cell types. *Biotechnol Bioeng* 2003; 83: 173–180.
36. Beachley V, Katsanevakis E, Zhang N, et al. A novel method to precisely assemble loose nanofiber structures for regenerative medicine applications. *Adv Healthc Mater* 2013; 2: 343–351.
37. Jakab K, Norotte C, Damon B, et al. Tissue engineering by self-assembly of cells printed into topologically defined structures. *Tissue Eng Part A* 2008; 14: 413–421.
38. Norris RA, Damon B, Mironov V, et al. Periostin regulates collagen fibrillogenesis and the biomechanical properties of connective tissues. *J Cell Biochem* 2007; 101: 695–711.
39. Hajdu Z, Mironov V, Mehesz AN, et al. Tissue spheroid fusion-based in vitro screening assays for analysis of tissue maturation. *J Tissue Eng Regen Med* 2010; 4: 659–664.
40. Sidhu SS, Yuan S, Innes AL, et al. Roles of epithelial cell-derived periostin in TGF-beta activation, collagen production, and collagen gel elasticity in asthma. *Proc Natl Acad Sci U S A* 2010; 107: 14170–14175.
41. Robinson EE, Foty RA and Corbett SA. Fibronectin matrix assembly regulates alpha5beta1-mediated cell cohesion. *Mol Biol Cell* 2004; 15: 973–981.
42. Robinson EE, Zazzali KM, Corbett SA, et al. Alpha5beta1 integrin mediates strong tissue cohesion. *J Cell Sci* 2003; 116: 377–386.
43. Montesano R and Orci L. Transforming growth factor beta stimulates collagen-matrix contraction by fibroblasts: implications for wound healing. *Proc Natl Acad Sci U S A* 1988; 85: 4894–4897.
44. Tomasek JJ, Gabbiani G, Hinz B, et al. Myofibroblasts and mechano-regulation of connective tissue remodelling. *Nat Rev Mol Cell Biol* 2002; 3: 349–363.
45. Tibbits S. 4D printing: multi-material change. *Architect Des* 2014; 84: 161–121.